1-1-2009

Extremely large post-liquefaction deformations of saturated sand under cyclic torsional shear loading

Gabriele Chiaro
University of Wollongong, gchiaro@uow.edu.au

Takashi Kiyota
University Of Tokyo, kiyota@iis.u-tokyo.ac.jp

Laddu Indika Nalin De Silva
University of Moratuwa

Takeshi Sato
Integrated Geotechnology Institute Ltd., tsato@iis.u-tokyo.ac.jp

Junichi Koseki
University Of Tokyo, koseki@iis.u-tokyo.ac.jp

EXTREMELY LARGE POST-LIQUEFACTION DEFORMATIONS OF SATURATED SAND UNDER CYCLIC TORSIONAL SHEAR LOADING

Gabriele CHIARO[1], Takashi KIYOTA[2], Laddu Indika Nalin DE SILVA [3], Takeshi SATO[4] and Junichi KOSEKI[5]

ABSTRACT

The effect of static shear stress on the undrained cyclic behavior of saturated Toyoura sand was studied by conducting a series of torsional shear tests up to double amplitude shear strain of about 100%. After being isotropically consolidated, the specimens were subjected to drained monotonic torsional shear loading, and then, cyclic torsional shear stress was applied under undrained condition. The amplitude of combined static and cyclic shear stress was kept constant by correcting the measured value for the effect of membrane force. Based on these test results, it was found that the effective stress path and the stress-strain curve were affected by the initial static shear stress. Accumulation of shear strain was clearly noticed in the same direction where the static shear stress was applied. Localization of specimen deformation, which increases with the shear strain level, was observed.

Keywords: Large strain, Liquefaction, Membrane force, Sand, Static shear stress, Torsional shear test

INTRODUCTION

During past earthquake events, such as the 1964 Niigata and 1983 Nihonkai-Chubu earthquakes, extremely large deformations could be observed on liquefied gentle slope of sand (Hamada et al., 1994). Even though the gradient of slopes was merely of some percents, their lateral spreading achieved several meters. Due to liquefaction, flow of slope can occur when the mobilized shear stress of soil in its liquefied state exceeds the shear stress required for the static equilibrium of soil mass. Once deformations produced by flow liquefaction are triggered, they may become extremely large depending on the acting static shear stress.

Vaid and Finn (1979) studied the role of initial static shear stress on the resistance to liquefaction of Ottawa sand under cyclic simple shear conditions. It was found that resistance of liquefaction, measured by the cyclic shear stress amplitude, can decrease or remain unchanged with increase in initial static shear stress level.

To investigate the influence of static shear on undrained cyclic loading behavior of Ottawa sand, Vaid and Chern (1983) carried out triaxial tests on samples anisotropically consolidated to various principal stress ratios. Based on the test results, it was shown that resistance to liquefaction can increase or decrease with increasing static shear stress level depending on relative density. It was also shown that flow deformation occurs during cyclic loading on loose sand and is responsible for reduced resistance to straining in loose sample with higher initial static shear stress.

In order to evaluate the characteristics of cyclic shear strength and residual deformation of saturated sand with initial static shear stress subjected to cyclic loading, Hyodo et al. (1991) performed undrained cyclic triaxial compression tests by using isotropically and anisotropycally consolidated specimens. The behavior of each sample was classified into three types: stress reversal,

[1] PhD Student, Department of Civil Engineering, The University of Tokyo, Japan, chiaroga@iis.u-tokyo.ac.jp
[2] Assistant Professor, Tokyo University of Science, Japan, kiyo@rs.noda.tus.ac.jp
[3] Post Doctoral Research Fellow, Institute of Industrial Science (IIS), The University of Tokyo, Japan, nalin@iis.u-tokyo.ac.jp
[4] Research Support Promotion Member, IIS, The University of Tokyo, Japan, tsato@iis.u-tokyo.ac.jp
[5] Professor, IIS, The University of Tokyo, Japan, koseki@iis.u-tokyo.ac.jp

no reversal and intermediate. The pattern of failure was distinguished into two kinds, liquefaction and resiadual deformation based on the difference in the effective stress paths and the modes of development of cyclic residual axial strain. In the cases of stress reversal and intermediate on loose samples, failure was associated with liquefaction, while in the other case it was found that residual deformation brought the sample to failure even though no liquefaction occurred; failure was not observed in the case of no reversal on dense sample.

However, in all of the above studies, due to mechanical limitation of the employed apparatus the shear strain level could not exceed 10% in case of simple shear tests; while regarding to triaxial tests, axial strain level was limited to 20% or less, due to large extents of non-uniform deformation of the specimen at higher strain levels.

Since the soil in a sloping ground is always subjected to an initial driving shear stress prior to seismic loading, and because properties of liquefied soil under extremely large deformation are still not clearly understood, in the present study, in order to investigate the effect of initial static shear stress level on the undrained cyclic behavior of saturated Toyoura sand, a series of undrained reversal cyclic torsional shear tests was performed up to double amplitude of shear strain of about 100%.

TEST APPARATUS

To achieve extremely large torsional shear displacements, a torsional test apparatus on hollow cylindrical specimens (Fig.1), developed by Koseki et al. (2007) and Kiyota et al. (2008), was employed in this study.

This apparatus is capable of achieving double amplitude torsional shear strain levels exceeding 100% by using a belt-driven torsional loading system that is connected to an AC servo motor through electro-magnetic clutches and reduction gears.

To measure large torsional deformations, a potentiometer with a wire and a pulley was employed, as shown in Figs. 1b) and 1c). The torque and axial load were detected by using a two-component load cell which is installed inside the pressure cell.

The hollow cylindrical specimen was 150mm in outer diameter, 90mm in inner diameter and 300mm in height.

TEST PROCEDURE

The material was Toyoura sand, uniform sand with negligible fine contents under 75μm (Table 1). Several specimens, as listed in Table 2, were prepared by pluviation air-dried sand particles through air. Their initial relative density of about 40-45% was obtained by using a funnel and keeping constant the height of pluviation.

After saturating the specimens with pouring carbon dioxide and then pouring de-aired water, they were isotropically consolidated by increasing the effective stress state up to 100kPa, with a back pressure of 200kPa. Then, the stress state was changed by applying drained monotonic torsional shear stress up to a specified value. Finally, undrained cyclic torsional loading, with constant double amplitude of shear stress of 32kPa, was applied at a constant shear strain rate of 2.5 %/min. The loading direction was reversed when the amplitude of combined shear stress, which was corrected for the effect of membrane force, reached the target value. For all the duration of torsional loading, both monotonic and cyclic cases, the vertical deformation of the specimen was kept to be zero by using a mechanical locking devices for the vertical displacement of loading shaft.

Table 1. Material properties

Material	Specific gravity, G_s	Maximum void ratio, e_{max}	Minimum void ratio, e_{min}	Mean diameter, D_{50} (mm)	Fines content, F_C (%)
Toyoura sand	2.656	0.992	0.632	0.16	0.1

Table 2. Test conditions

Test	Relative density, D_r	Static Shear Stress, τ_S	Combined shear stress, $\tau_S \pm \tau_{CL}$	Type of loading
Test SH00	40.5%	0kPa	+16/-16kPa	Reversal
Test SH03	45.1%	3kPa	+19/-13kPa	Reversal
Test SH05	43.3%	5kPa	+21/-11kPa	Reversal
Test SH10	44.3%	10kPa	+ 26/-6kPa	Reversal
Test SH15	41.9%	15kPa	+ 31/-1kPa	Reversal
Test SH16	44.2%	16kPa	+32/0kPa	Intermediate
Test SH20	43.2%	20kPa	+36/+4kPa	Non-reversal

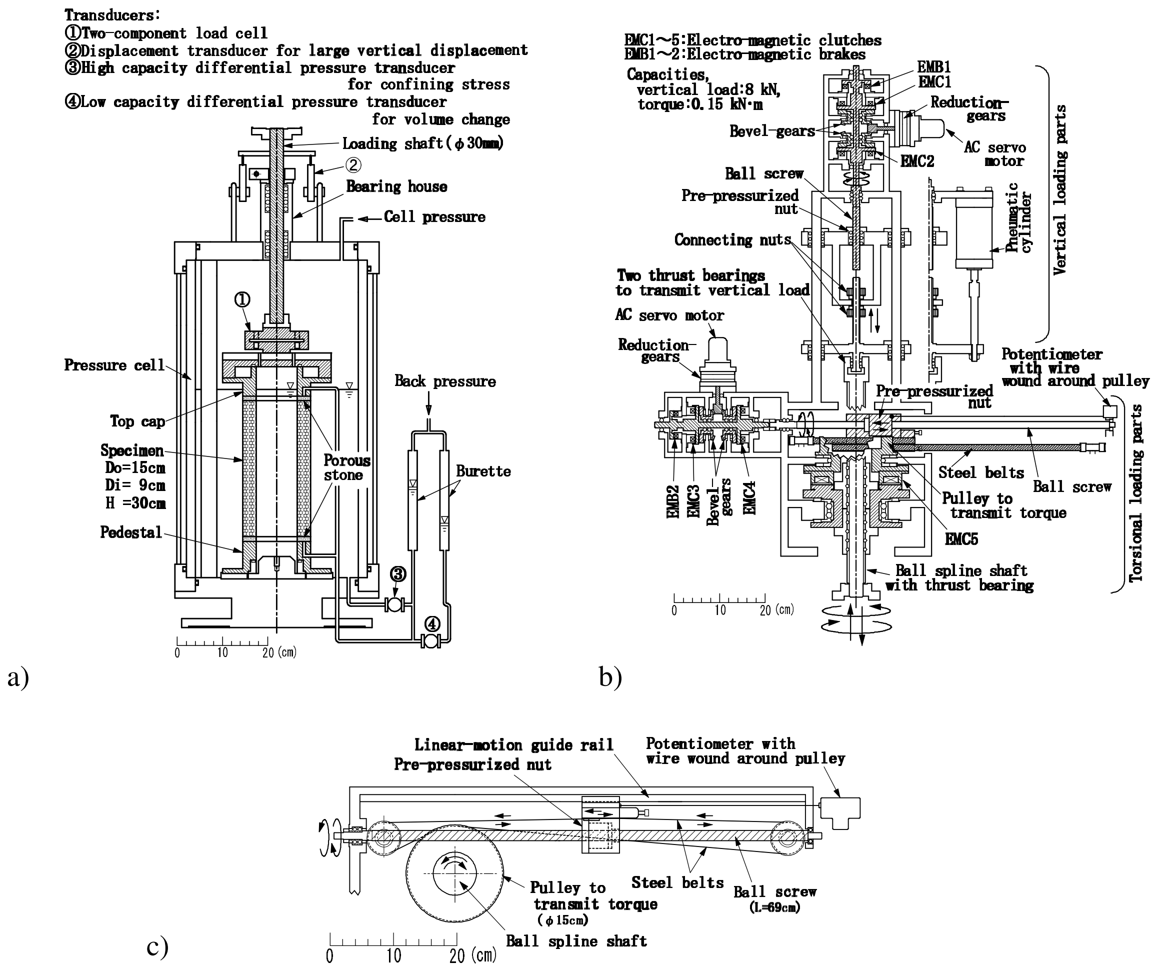

Figure 1. a) Torsional shear test apparatus on hollow cylindrical specimen; b) loading device and c) plan view of torque-transmission part (after Kiyota et al., 2008)

TEST RESULTS

Correction for membrane force

As Koseki et al. (2007) among others indicated, in torsional shear tests on hollow cylindrical specimen due to the presence of inner and outer membranes, the effect of membrane force can not be neglected. In addition, it becomes significantly important when shear strain reach extremely high level as Kiyota et al. (2008) reported.

Usually, the membrane force has been corrected based on the linear elasticity theory, which uses the Young's modulus of the membrane. The theoretical apparent shear stress, τ_m, induced by the inner and outer membranes can be evaluated as:

$$\tau_m = \frac{t_m \, E_m \left(r_o^3 + r_i^3\right)\theta}{\left(r_o^3 - r_i^3\right)h} \tag{1}$$

where θ is the rotational angle of the top cap detected by external potentiometer; h is the height of the specimen; r_o and r_i are the outer and inner radii of the specimen; t_m and E_m are, respectively, the thickness (=0.3 mm) and the Young's modulus (=1492kPa) of membrane.

In order to confirm the validity of Eq. (1) in correcting for the effect of membrane force, a special test was performed by filling water between the inner and outer membranes and shearing it cyclically under undrained condition up to double amplitude shear strain of 100%.

Figure 2 shows both experimental and theoretical relationships between shear strain and apparent shear stress that is induced by the membranes due to torsional deformation. The deviation of the actual membrane deformation from the uniform one that is assumed in the theory became larger with increase in the strain level. Hence, in this study, the shear stress was corrected for the effect of membrane force by employing the polynomial approximation of the measured relationship between γ and τ_m as shown in Fig. 2.

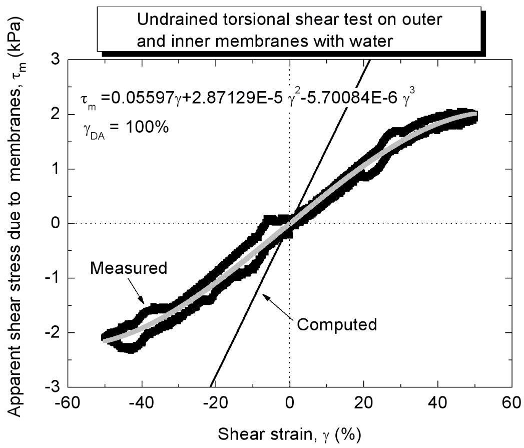

Figure 2. Relationships between apparent shear stress due to membrane force and shear strain

Test results

Reversal loading tests

During each cycle of loading in some tests, the combined static and cyclic shear stress value is reversed from positive ($\tau = \tau_S + \tau_{CL} > 0$) to negative ($\tau = \tau_S - \tau_{CL} < 0$), or vice versa; by using the classification introduced by Hyodo et al. (1991), this type of loading will be called hereafter as reversal loading.

Typical stress reversal loading test results on Toyoura sand specimens, in which there is no static shear stress ($\tau_S = 0$), are shown in Fig 3. In addition, Figs. 4 trough 7 show results of tests in which static shear stress with magnitude of 3, 5, 10 and 15kPa, respectively, was applied before undrained torsional loading.

Cyclic mobility was observed in Figs. 3a), 4a), 5a), 6a) and 7a) where the effective stress recovered repeatedly after achieving the state of zero effective stress (i.e., liquefaction). It was accompanied with a significant development of double amplitude shear strain, γ_{DA}, as shown in Figs. 3b), 4b), 5b) , 6) and 7b).

From the comparison of the effective stress paths, it was observed that by increasing the initial amount of static shear stress, saturated sand becomes much more resistant to liquefaction up to certain level (i.e., the number of cycles to cause liquefaction increased with the increase in the static shear stress). On the other hand, when the static shear stress becomes too large, liquefaction easily occurs with less number of cycles.

In the post-liquefaction state, the shear strain increased with the number of cycles; this process clearly depended on the applied static shear stress, in the sense that accumulation of shear strain was noticed in the same direction where the previously monotonic drained shear stress was applied.

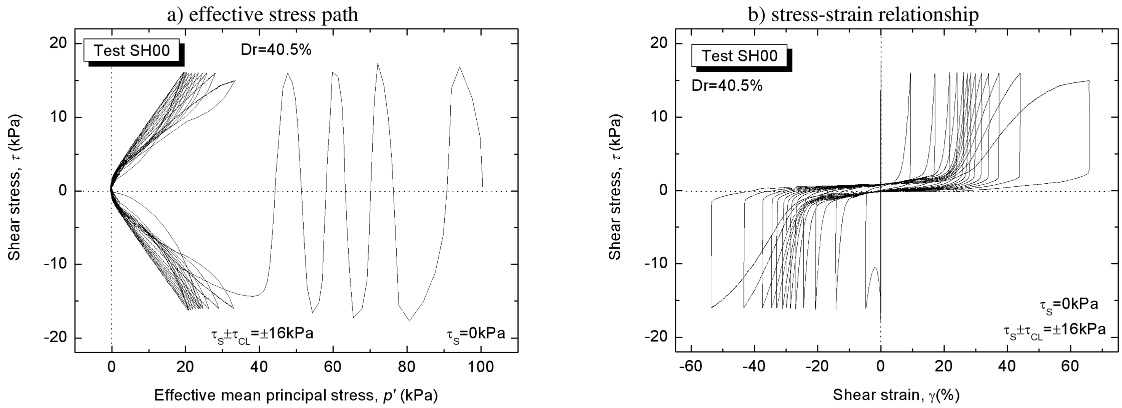

Figure 3. Typical test results on Toyoura sand without applying any static shear stress (τ_S=0)

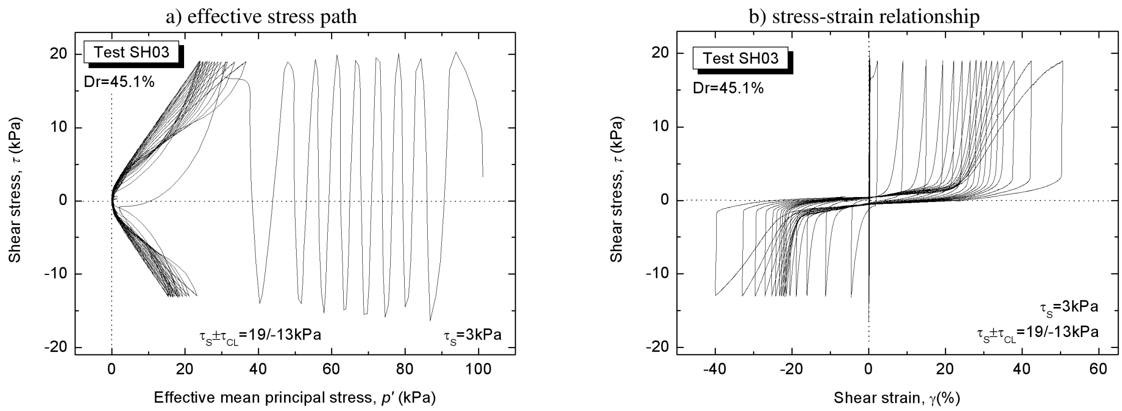

Figure 4. Typical test result on Toyoura sand applying static shear stress (τ_S=3kPa)

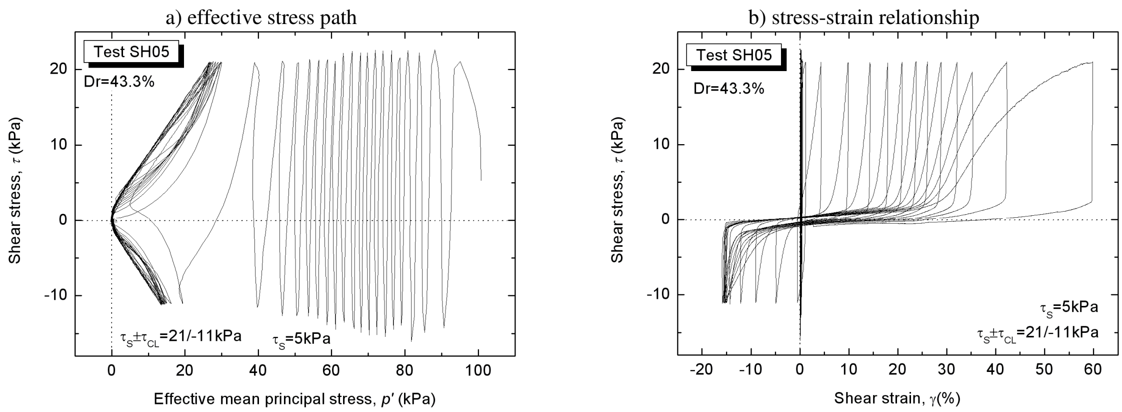

Figure 5. Typical test results on Toyoura sand applying static shear stress (τ_S=5kPa)

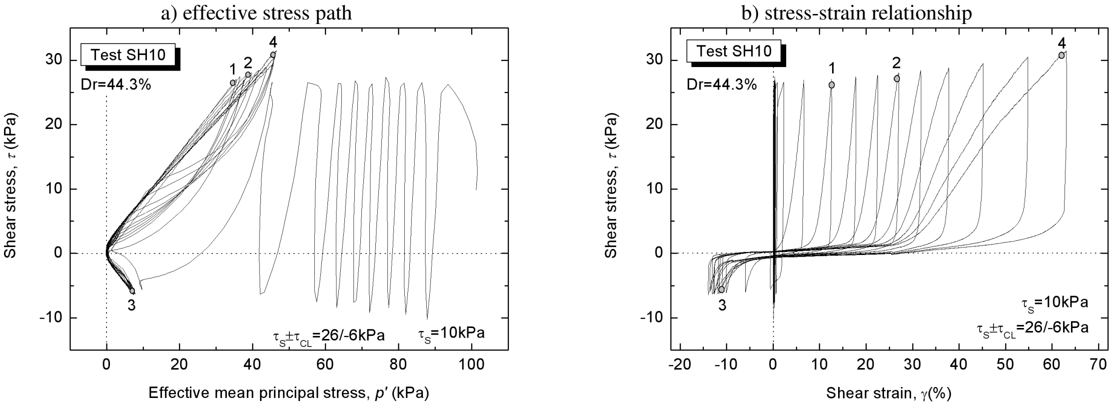

Figure 6. Typical test results on Toyoura sand applying static shear stress (τ_S=10kPa)

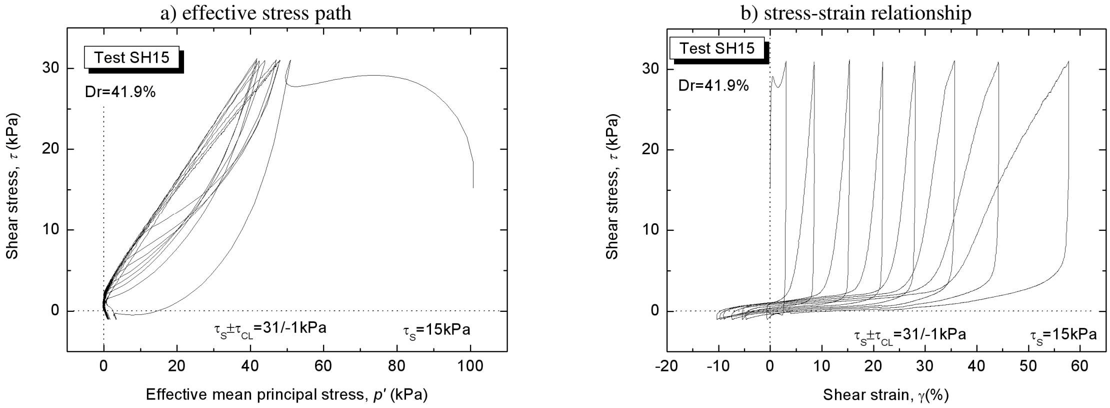

Figure 7. Typical test results on Toyoura sand applying static shear stress (τ_S=15kPa)

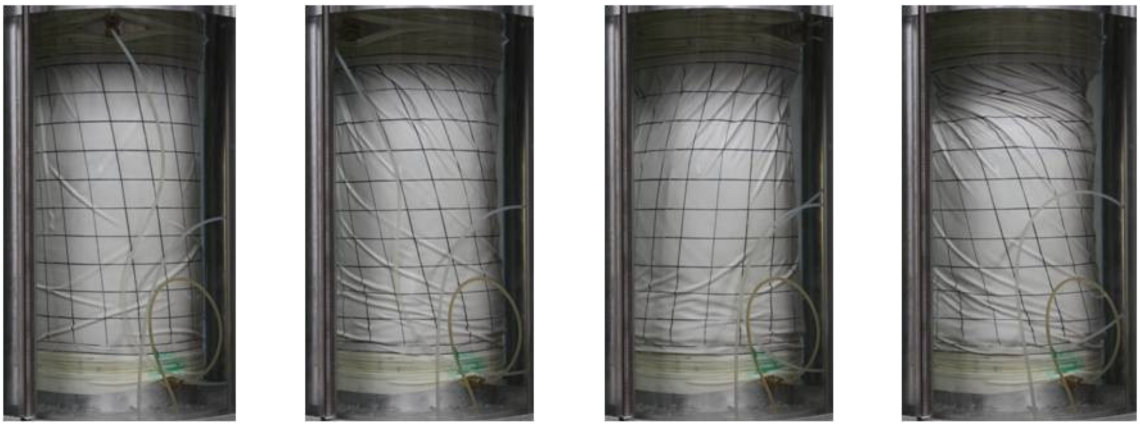

a) state 1 (γ=12%) b) state 2 (γ=27%) c) state 3 (γ=-11%) d) state 4 (γ=63%)

Photo 1. Specimen deformation at states 1 through 4 shown in Fig. 6

Specimen deformation at several states as numbered 1 through 4 in Fig. 6 is shown in Photo 1. At state 1 (γ= 12%), the deformation was almost uniform except for the regions close to the pedestal and the top cap that are affected by the end restraint; the outer membrane appeared slightly wrinkled. At state 2 (γ= 27%), the outer membrane was visibly wrinkled; in the region near the top cap the deformation of the specimen started to localize due possibly to formation of water film. At state 3 (γ= -11%), the localization of specimen deformation developed clearly in the upper part of the specimen. At state 4 (γ=63%), the specimen was almost twisted near the top cap.

Intermediate and non-reversal loading tests

In accordance with the classification introduced by Hyodo et al. (1991), herein, the type of loading in which the reversal of loading direction is made when combined shear stress (static + cyclic, $\tau_S \pm \tau_{CL}$) achieves zero state during the undrained torsional shear loading is called intermediate loading and the one in which the combined shear stress is always kept positive is called non-reversal loading.

Fig. 8 shows typical test results with intermediate loading, whereas Fig. 9 shows the case with non-reversal loading.

In case of intermediate loading test, liquefaction was accompanied by cyclic mobility (Fig. 8a)) with a significant development of shear strain as shown in Fig. 8b). It should be noticed that, in a different way from the reversal loading case, in this test progressive large deformation was developed during each cycle without recovering zero or negative shear strain state.

As indicated in Fig 9a), in case of non-reversal loading, the state of zero effective stress was not reached even after applying 208 cycles. Fig. 9b) shows that large shear strain level exceeding 50% was achieved, even though the zero effective stress state did not occur.

a) effective stress path b) stress-strain relationship

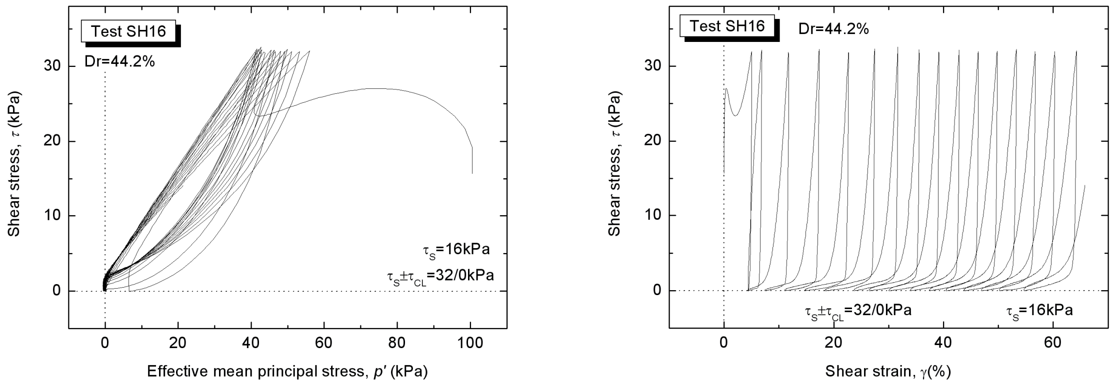

Figure 8. Intermediate loading test results on Toyoura sand (τ_S=16kPa)

a) effective stress path b) stress-strain relationship

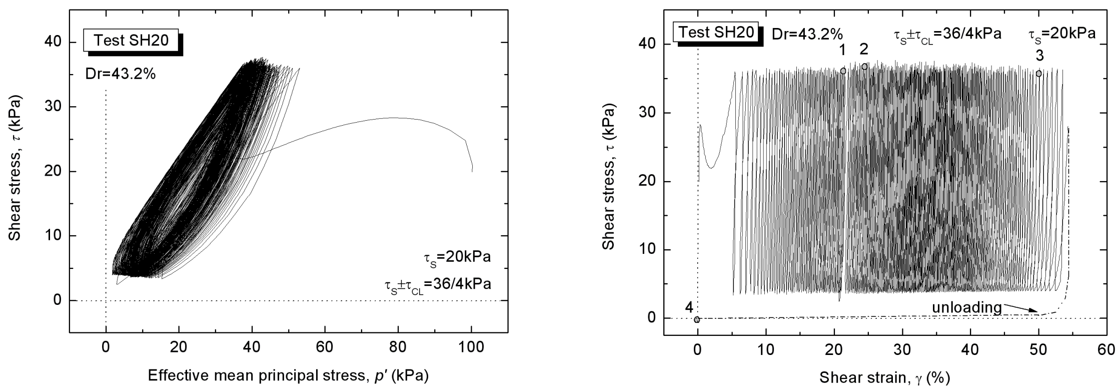

Figure 9. Non-reversal loading test results on Toyoura sand (τ_S=20kPa)

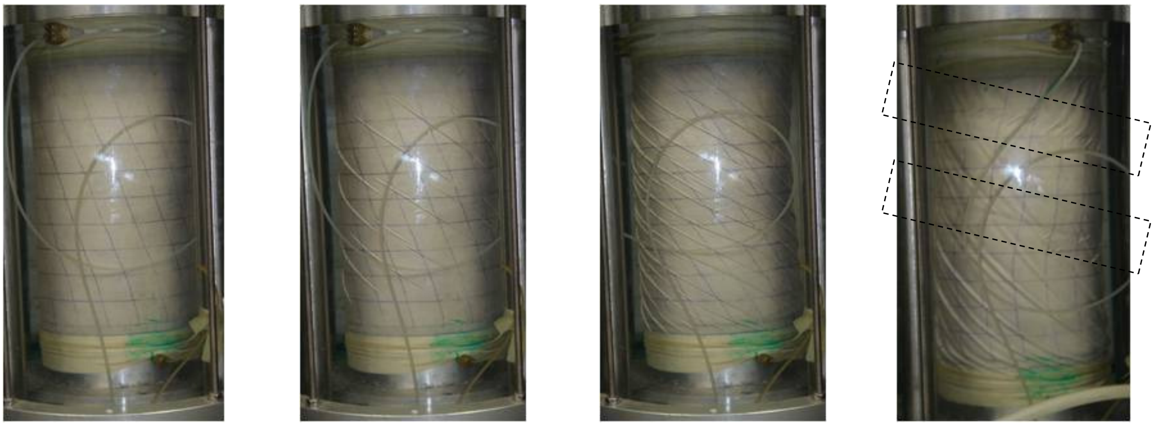

a) state 1 (γ=21%) b) state 2 (γ=25%) c) state 3 (γ=50%) d) state 4 (after test)

Photo 2. Specimen deformation at states 1 through 3 shown in Fig. 9

Specimen deformation at several states as numbered 1 through 4 in Fig. 9 is shown in Photo 2. At state 1 (γ=21%) the deformation was rather uniform except for the zones near the top cap and pedestal due to the effect of end restraint. At state 2 (γ=25%) the outer membrane was wrinkled at several locations due possibly to local drainage. At state 3 (γ=50%) the membrane was extensively wrinkled from the bottom to the top. At state 4 (after unloading to zero shear stress state while keeping undrained condition), formation of a spiral shear band could be observed (Photo 2d)).

The results of this non-reversal loading test indicate that, when the combined shear stress can not reach zero state, liquefaction (i.e., the zero effective stress state) does not occur. However, this does not mean that sand is very resistant against seismic loading, in fact a significant magnitude of combined shear stress may cause failure as evidenced with the formation of shear band.

Effect of initial static shear stress on cyclic behavior of saturated sand

In this study, the effect of initial static shear stress on cyclic behavior of saturated Toyoura sand was examined in terms of the relationships between the cyclic stress ratio defined as $(\tau_S+\tau_{CL})/p_0'$ and the number of cycles to cause liquefaction (i.e., the effective stress state) or specific amounts of shear strain, as listed in Table 3.

Table 3. Number of cycles required to cause liquefaction or specific amounts of shear strain

Test	Cyclic stress ratio $(\tau_S+\tau_{CL})/p_0'$	Liquefaction	γ=10%	γ=20%	γ=30%	γ=40%	γ=50%
Test SH00	0.16	4	5	7	13	16	17
Test SH03	0.19	9	12	14	19	24	25
Test SH05	0.21	20	23	26	30	32	33
Test SH10	0.26	10	13	15	17	19	20
Test SH15	0.31	2	3	4	6	7	8
Test SH16	0.32	3	3	5	7	10	13
Test SH20	0.36	No liquefaction	8	46	98	164	202
p_0'= initial effective mean principal stress (=100kPa)							

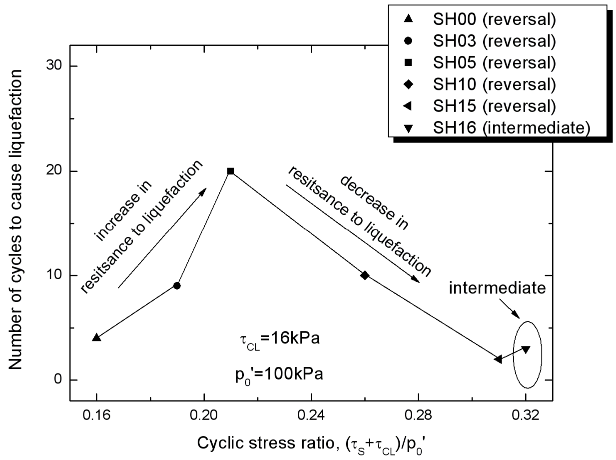

Figure 10. Effect of initial static shear stress on cyclic stress ratio required to cause liquefaction

As indicated in Fig.10, the resistance to liquefaction of saturated sand can increase or decrease with increase in initial static shear stress depending on the magnitude of cyclic stress ratio and the type of loading (i.e., reversible or intermediate loading). The number of cycles required to cause liquefaction increases with the amount of initial static shear stress up to a threshold value of cyclic stress ratio; then, after exceeding this critical value, liquefaction easily occurs with less cycles. In addition, another change in sand behavior can be observed when the type of loading changes from reversal to intermediate, in the sense that resistance to liquefaction slightly increase. In case of stress no reversal loading liquefaction does not occur.

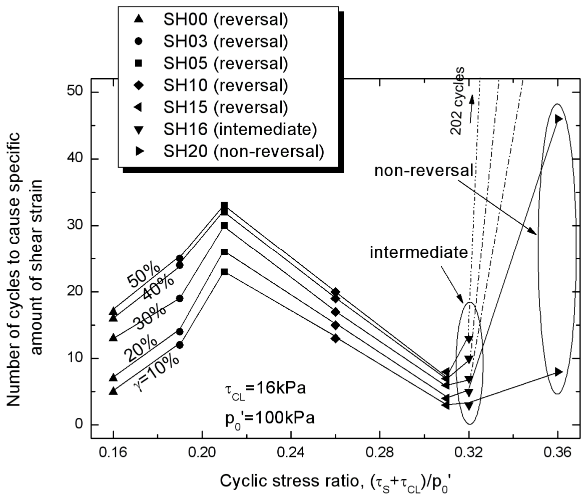

Figure 11. Effect of initial static shear stress on cyclic stress ratio required to cause 10%, 20%, 30%, 40% and 50% of shear strain

After achieving the state of zero effective stress (i.e., liquefaction), a significant accumulation of shear strain occurs while showing cyclic mobility. Fig.11 shows the number of cycles required to cause specific amounts of shear strain. This number of cycles can increase or decrease with increase in initial static shear stress depending on the magnitude of cyclic stress ratio and the type of loading (i.e., reversible, intermediate or non-reversal loading). The resistance to strain accumulation increases with increasing the cyclic stress ratio up to a threshold value; after exceeding this value, large shear strain level can be developed with smaller number of cycles. The lower resistance to strain accumulation in loose specimens with higher initial static shear stress may be associated with the occurrence of flow failure as Vaid and Chern (1983).

In Fig. 11, it can be also observed that soil becomes stronger when the type of loading changes from reversal to intermediate, and much more in the case of non-reversal loading because liquefaction does not occur.

CONCLUSIONS

The results from a series of undrained cyclic torsional shear tests, conducted on saturated Toyoura sand specimens up to extremely large deformation, can be summarized as follows:

1) By using the modified torque loading devices, undrained cyclic torsional tests could be conducted on saturated Toyoura sand up to double amplitude shear strain of about 100%.
2) In using hollow cylindrical specimens, due to the presence of inner and outer membranes, correction for effect of membrane force on the measured value of shear stress is indispensable.
3) Both the effective stress path and the stress-strain curve were affected by the initial value of static shear stress. In particular, reversal loading tests revealed that, by increasing the initial amount of static shear stress, large shear strain levels could develop with less cycles.
4) Saturated loose Toyoura sand undergoing cyclic torsional shear stress behaved in two different ways depending on the value of combined shear stress (static + cyclic). In case of reversal and intermediate loadings, the sand liquefied and large deformation was developed while showing cyclic mobility. On the other hand, in case of non-reversal loading, liquefaction did not occur, and under large shear strain levels formation of shear bands was clearly observed.
5) Accumulation of shear strain was clearly noticed in the same direction where previously monotonic drained shear stress was applied.
6) In the case of reversal loading, progressive localization of specimen deformation was observed clearly in the region near the top cap where the specimen was almost twisted due to possibly water film formation; whereas, in the case of non-reversal loading, due to possibly local drainage the outer membrane was extensively wrinkled along the whole specimen height.
7) The resistance to liquefaction and the resistance to strain accumulation can increase or decrease with increasing initial static shear stress depending on the magnitude of cyclic stress ratio and the type of loading.

REFERENCES

Hamada, M., O'Rourke, T.D. and Yoshida, N. (1994): Liquefaction-induced large ground displacement, *Performance of Ground and Soil Structures during Earthquakes, 13th ICSMFE*, *JGS*, 93-108

Hyodo, M., Murata, H., Yasufuku, N. and Fujii, T. (1991): Undrained cyclic shear strength and residual shear strain of saturated sand by cyclic triaxial tests, *Soils and Foundations*, 31(3), 60-76

Kiyota, T., Sato, T., Koseki, J., and Mohammad, A. (2008): Behavior of liquefied sands under extremely large strain levels in cyclic torsional shear tests, *Soils and Foundations*, 48(5), 727-739

Koseki, J., Kiyota, T., Sato, T. and Mohammad, A.M. (2007): Undrained cyclic torsional shear tests on sand up to extremely large strain levels, *International Workshop on Earthquake Hazard and Mitigation, Guwahati, India, 7-8 December 2007,* 257-263

Vaid, Y.P. and Finn, W.D.L. (1979): Static shear and liquefaction potential, *Journal of the geotechnical Engineering Division, Proc. ASCE*, Vol.105, GT10, 1233-1246

Vaid, Y.P. and Chern, J.C. (1983): Effects of static shear on resistance to liquefaction, *Soils and Foundations*, 23(1), 47-60